A coupled modelling approach for the fast computation of underwater noise radiation from offshore pile driving

Peng, Yaxi; Tsouvalas, Apostolos; Metrikine, Andrei V.

DOI
10.47964/1120.9196.18574

Publication date
2020

Document Version
Final published version

Published in
EURODYN 2020 XI International Conference on Structural Dynamics

Available online at www.easdprocedia.org
EASD Procedia EURODYN (2020) 2427-2436

EASD Procedia

EURODYN 2020
XI International Conference on Structural Dynamics
M. Papadrakakis, M. Fragiadakis, C. Papadimitriou (eds.)
Athens, Greece, 23–26 November 2020

A COUPLED MODELLING APPROACH FOR THE FAST COMPUTATION OF UNDERWATER NOISE RADIATION FROM OFFSHORE PILE DRIVING

Yaxi Peng[1], **Apostolos Tsouvalas**[1], **Andrei V. Metrikine**[1]

[1]Delft University of Technology
Faculty of Civil Engineering and Geosciences
Stevinweg 1, 2628CN Delft, The Netherlands
e-mail: {y.peng, a.tsouvalas, a.metrikine}@tudelft.nl

Keywords: underwater noise, offshore pile driving, vibro-acoustics, noise propagation, offshore wind.

Abstract. *This paper presents a computationally efficient modelling approach for the prediction of underwater noise radiation from offshore pile driving. A near-source module is adopted to capture the interaction between the pile, fluid and soil, which is based on a previously developed semi-analytical vibro-acoustic model. This module primarily aims at modelling the sound generation and propagation in the vicinity of the monopile. The Green's tensor for an axisymmetric ring source in a horizontally stratified acousto-elastic half-space emitting both compressional and shear waves is derived using the normal modes and branch line integrations. The boundary integral equations are then formulated based on the reciprocity theorem, which forms the mathematical basis of the far-from-source module for the propagation of the wave field at large radial distances. The complete noise prediction model comprises the two modules, which are coupled through the boundary integral formulation with the input obtained from the near-source module. Model predictions are benchmarked against measurement data from an offshore installation campaign.*

ISSN:2311-9020
Peer-review under responsibility of the Organizing Committee of EURODYN 2020.
doi: 10.47964/1120.9196.18574

1 INTRODUCTION

The anthropogenic noise generated during the installation of the foundation piles for offshore wind farms has raised serious concern over environmental issues. The underwater noise pollution can endanger the lives of marine mammals and fishes [1]. Under the strict environmental regulations imposed by the government in many countries, the offshore industry strives to keep the noise levels to within acceptable limits. To assess the noise levels to be expected and control the hydro-sound emission, underwater noise predictions are required prior to the offshore installation of piles in most projects.

Over the last decades, modeling of the underwater noise generated by offshore pile driving has been studied extensively. Reinhall and Dahl [2] firstly proposed a coupled Finite Element (FE) and Parabolic Equation (PE) model for the prediction of underwater noise for offshore pile driving. The former method (FE) aims at generating the noise in the vicinity of the pile, while the latter one (PE) focus on the long-range propagation of the sound field. The coupling is achieved via a vertical array of phased point sources from FE results. Lippert and Estorff [3] presented a coupled FE and wavenumber integration model and investigated the influence of uncertainties in the sediment parameters through Monte-Carlo simulations. A theoretical benchmark case was then examined by various models discussed in [4]. Similar to [2], a two-step approach is adopted in most available models mentioned in [4, 3, 5] with a FE model to capture the vibration of the pile and a sound propagation model to propagate the field at larger distances (from the pile).

A semi-analytical approach for the prediction of underwater noise from pile driving was developed by Tsouvalas and Metrikine [6] based on a mode-matching technique. In contrast to most of the aforementioned models, this model additionally captured the characteristics of more complex seabed conditions with the soil being described as a three-dimensional elastic continuum. This allows one to examine the influence of the seabed properties on the noise generation and transmission.

In this paper, the authors present a coupled modelling approach for the noise prediction by impact piling with the focus being placed on a computationally efficient approach for the propagation of the sound field at large distances. The method extends the earlier works [7] by a far-range propagation module. The complete model comprises two modules: i) a near-source module aiming at the accurate description of the pile-water-soil interaction together with the sound generation and propagation in the pile vicinity [6], and ii) a far-from-source module aiming at the propagation of the wavefield at larger distances. The input to the far-from-source module is provided by the near-source module through the boundary integral formulation.

Section 2 introduces the mathematical statement of the problem together with the solution technique. In section 3, an experimental benchmark case is presented and measurement results are compared to model predictions. Finally, section 4 gives an overview of the main conclusions of the paper.

2 THEORY

The complete vibro-acoustic model for noise prediction in impact piling is shown in Fig.1. The pile is modelled as linear elastic thin shell occuping the domain $0 \leq z \leq L$. A vertical force $F(t)$ is applied at the top side of the pile. The ocean environment is modelled as an acousto-elastic layered waveguide. The fluid is modelled as a three-dimensional inviscid compressible medium with a compressional wave speed c_f and a density ρ_f occupying the domain $z_0 \leq z \leq z_1$ and $r \geq R$. The soil is described as a three-dimensional horizontally stratified elastic

continuum. Each soil layer is characterised by its density ρ_j, the compressional and shear wave speeds $c_{p,j}$ and $c_{s,j}$, and the compressional and shear damping coefficients $\alpha_{p,j}$ and $\alpha_{s,j}$, respectively. In the near-source module, the soil occupies the domain $z \geq z_1$ and is terminated at a large depth $z = H$ with a rigid boundary which has been shown not to affect the pile vibrations and noise generation in the vicinity of the pile [6]. In the far-from-source module, the soil extends to infinity in the vertical direction to accurately capture the energy loss mechanisms at larger distances from the pile.

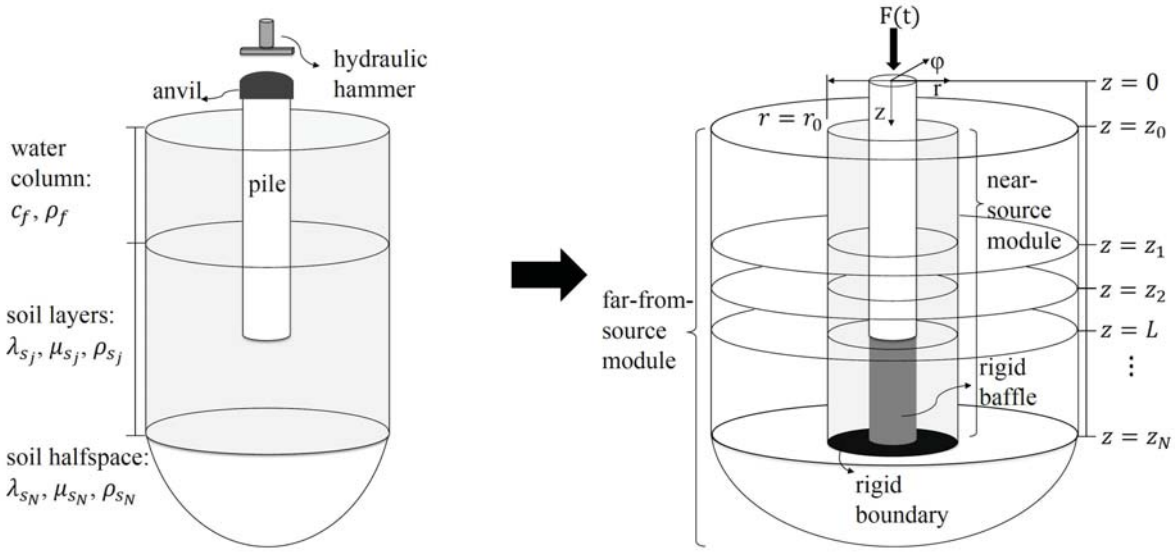

Figure 1: Geometry of the complete system (left) and the coupled modelling approach (right).

2.1 Governing equations

The equations of motion of the pile-soil-water system read [7]:

$$\mathbf{L}\,\mathbf{u}_p + \mathbf{I}_m\,\ddot{\mathbf{u}}_p = -\left[H(z-z_0) - H(z-L)\right]\,\mathbf{t}_s + \mathbf{f} \tag{1}$$

$$G_j\,\nabla^2\mathbf{u}_s^j + (\lambda_j + G_j)\,\nabla\nabla\cdot\mathbf{u}_s^j - \rho_j\ddot{\mathbf{u}}_s^j = \mathbf{0} \tag{2}$$

$$\nabla^2\phi_f(r,z,t) - \frac{1}{c_f^2}\ddot{\phi}_f(r,z,t) = 0 \tag{3}$$

In the equations above, $\mathbf{u}_p = [u_{p,z}(z,t)\ u_{p,r}(z,t)]^{\mathrm{T}}$ is the displacement vector of the mid-surface of the shell, $\mathbf{u}_s^j(r,z,t) = \left[u_{s,z}^j(r,z,t)\ u_{s,r}^j(r,z,t)\right]^{\mathrm{T}}$ is the displacement vector of each solid layer and $\phi_f(r,z,t)$ is a velocity potential introduced for the description of the fluid. The operators $\mathbf{L}$ and $\mathbf{I}_m$ are the stiffness and modified inertia matrices, respectively [6]. The vector $\mathbf{t}_s$ represents the boundary stress vector that takes into account the reaction of the soil and fluid surrounding the shell at $z_0 < z < L$. Naturally, in the domain $z_0 < z < z_1$ this reflects only the normal pressure exerted by the fluid normal to the surface whereas for $z > z_1$ both shear and normal stresses are present. The functions $H(z - z_i)$ are the Heaviside step functions which are used here to account for the fact that the soil and the fluid are in contact with a segment

of the shell in correspondence with Fig.1. The vector $\mathbf{f} = [f_{rz}(z,t)\ f_{rr}(z,t)]^{\mathrm{T}}$ represents the externally applied force on the surface of the shell.

A set of boundary conditions and interface conditions are formulated as follows for $r \geq R$:

$$p_f(r, z_0, t) = 0 \tag{4}$$

$$\sigma^1_{s,zz}(r, z_1, t) + p_f(r, z_1, t) = 0,\ \sigma^1_{s,zr}(r, z_1, t) = 0,\ u^1_{s,z}(r, z_1, t) - v_{f,z}(r, z_1, t) = 0 \tag{5}$$

$$\sigma^{j+1}_{s,zi}(r, z_j, t) - \sigma^{j}_{s,zi}(r, z_j, t) = 0,\ u^{j+1}_{s,i}(r, z_j, t) - u^{j}_{s,i}(r, z_j, t) = 0\,,\ 2 \leq j \leq N-1,\ i = z, r \tag{6}$$

$$u^N_{s,r}(r, z_N, t) = u^N_{s,z}(r, z_N, t) = 0 \tag{7}$$

where $p_f(r, z, t)$ indicates the pressure in the fluid, $\sigma^j_{s,zi}(r, z, t)$ represents the stresses in the soil at the corresponent layer j. In addition to Eqs. (4–7), the radiation condition needs to be satisfied at $r \to \infty$. In the far-from-source module, the boundary conditions at $z = z_N$ are substituted by the radiation condition at $z \to \infty$, which indicates that the bottom soil is modelled as elastic half-space.

2.2 Solution to the coupled problem

The complete solution to the coupled vibroacoustic problem consists of two modules: (i) the near-source module aiming at the noise generation and propagation in the vicinity of the pile; and (ii) the far-from source module aiming at propagating the field at larger distances from the pile.

2.2.1 Near-source module

The near-source module is based on a three-dimensional vibroacoustic model developed by Tsouvalas and Metrikine [6]. The module captures the characteristic of dynamic interactions between the pile and the surrounding media. A modal decomposition is applied both for the shell structure and the acousto-elastic waveguide as:

$$\begin{aligned}
\tilde{u}_{p,k}(z, \omega) &= \sum_{m=1}^{\infty} A_m\, U_{km}(z)\,, \\
\tilde{\phi}_f(r, z, \omega) &= \sum_{p=1}^{\infty} C_p\, H_0^{(2)}(k_p r)\, \tilde{\phi}_{f,p}(z)\,, \\
\tilde{\phi}_s(r, z, \omega) &= \sum_{p=1}^{\infty} C_p\, H_0^{(2)}(k_p r)\, \tilde{\phi}_{s,p}(z)\,, \\
\tilde{\psi}_s(r, z, \omega) &= \sum_{p=1}^{\infty} C_p\, H_1^{(2)}(k_p r)\, \tilde{\psi}_{s,p}(z)\,,
\end{aligned} \tag{8}$$

in which the subscripts p, f, s indicate the pile structure, fluid and soil, respectively, k refers to the displacement components r and z, the index $m = 1, 2, ..., \infty$ represents the mode number.

$H_n^{(2)}$ denotes the n^{th}-order Hankel function of the second kind which ensures that the radiation condition at $r \to \infty$ is satisfied at all times. The expressions for the displacement and the pressure/stress fields can be obtained through Helmholtz decomposition by substituting the potential functions. The coefficients C_p with $p = 1, 2, ..., \infty$ are the unknown modal amplitudes. The coefficients A_m are the modal amplitudes to be determined by solving the coupled problem. The terms k_p denote the horizontal wavenumber obtained by the formulation of the eigenvalue problem of the acousto-elastic region [8]. A system of infinite algebraic equations to the unknown coefficients C_p can be obtained [7]:

$$\sum_{q=1}^{\infty} C_q \left(L_{qp} + k_q \, H_1^{(2)}(k_q R) \, \Gamma_q \, \delta_{qp} - \sum_{m=1}^{\infty} \frac{R_{mq} \, Q_{mp}}{I_m} \right) = \sum_{m=1}^{\infty} \frac{F_m \, Q_{mp}}{I_m} \tag{9}$$

The coefficients of the shell structure are given by:

$$A_m = \frac{F_m + \sum_{p=1}^{\infty} C_p \, R_{mp}}{I_m} \tag{10}$$

The terms L_{qp}, Γ_q, Q_{mp}, R_{mp} and I_m are computed given the expressions in [6], which are omitted here for brevity. The eigenproblem of the shell and the surrounding acousto-elastic medium can be solved independently, which provide flexibilities in examining various configurations of the system.

2.2.2 Far-from-source module

To propagate the axisymmetric disturbances radiated from the pile into the surrounding medium, Green's tensors for a ring source emitting both compressional and shear waves are first derived. Assuming that a ring source is positioned at $\boldsymbol{r}_0 = (r_0, z_0)$, the wave equation in the Fourier-Hankel domain reads [9]:

$$\left[\frac{d^2}{dz^2} + k_{z,\xi}^2 \right] \hat{\Phi}_{\Xi,\xi}^{g}(k_r, z; r_0, z_0, \omega) = \frac{J_0(k_r \, r_0)}{2\pi} \, \delta(z - z_0) S_{\beta}^{\xi}(\omega) \tag{11}$$

in which ξ indicates the type of the sources considered; "f" being a fluid source, "p" a compressional source, and "s" being a shear source. The subscript Ξ represents the position of the receiver in the layered medium. $S_{\beta}^{\xi}(\omega)$ represents the source strength, which will be determined based on a unit impulse in β direction at source point $\boldsymbol{r}_0$ as discussed in section 2.2.3.

The solutions to Eq.(11) for the displacement potentials $\hat{\Phi}_{\Xi,\xi}^{g} = [\hat{\phi}_{f,\xi}^{g}, \hat{\phi}_{s,\xi}^{g}, \hat{\psi}_{s,\xi}^{g}]$ in the wavenumber domain are first derived for an acousto-elastic layered half-space. Applying the inverse Hankel transform yields:

$$\tilde{\Phi}_{\Xi,\xi}^{g}(\boldsymbol{r}; \boldsymbol{r}_0, \omega) = -\frac{1}{2} \int_{-\infty}^{+\infty} (S_{\beta}^{\xi}(\omega) \frac{e^{-\mathrm{i}k_{z,\xi}|z-z_0|}}{4\pi \mathrm{i} k_{(}z,\xi)} + A_{\xi}^{1} e^{\mathrm{i}k_{z,\xi}z} + A_{\xi}^{2} e^{-\mathrm{i}k_{z,\xi}z}) J_0(k_r \, r_0) H_0^{(2)}(k_r \, r) k_r dk_r \tag{12}$$

For $z \geq z_N$, $A_{\xi}^{1} = 0$ to ensure that the downward propagating waves *leave* the soil half-space without reflection. Upon substitution of the Eq.(12) into Eqs.(4–6), it becomes clear that the kernels in the integral representations need to be satisfied. This yields a linear algebraic system of equations with unknowns A_{ξ}^{1} and A_{ξ}^{2}. Once the amplitude coefficients are solved for every

k_r, the Green's tensor for any configuration of compressional or shear source potentials can be obtained.

To evaluate the wavenumber integral given by Eq.(12), the complex contour integration technique is applied. The solution can be expressed as a summation of a finite number of (normal) modes supplemented by Ewing-Jardetsky-Press (EJP) branch line integrations. The final expression of the Green's tensor in modal summation for the acousto-elastic domain considered here reads:

$$\begin{aligned}\tilde{\Phi}^{g}_{\Xi,\xi}(r,z;r_0,z_0;\omega) &= -\pi i \sum_{m=1}^{M}\left[\frac{\hat{\Phi}^{g,num}_{\Xi,\xi}(k_r,z;r_0,z_0)}{f'(k_r)} J_0(k_r\, r_0) H_0^{(2)}(k_r r) k_r\right]^{(m)} \\ &+ \frac{1}{2}\int_{\alpha+\beta} \hat{\Phi}^{g}_{\Xi,\xi}(k_r,z;r_0,z_0) J_0(k_r\, r_0) H_0^{(2)}(k_r r) k_r dk_r\end{aligned} \tag{13}$$

in which $\hat{\Phi}^{g,num}_{\Xi,\xi} = [\hat{\phi}^{g,num}_{f,\xi}, \hat{\phi}^{g,num}_{s_j,\xi}, \hat{\psi}^{g,num}_{s_j,\xi}]$ denotes the numerator of the solutions of the potential functions in Hankel domain. The characteristic equation $f(k_r)$, being the determinant of the coefficient matrix, is used to determine the horizontal wavenumbers $k_r^{(m)}$.

2.2.3 Direct boundary element integral

The direct boundary element method (BEM) is adopted in this model to couple the near-source and far-from-source modules. The solution of the wavefield in both acoustic and elastodynamic field employs Somigliana's identity in elastodynamics and Green's third identity in potential theory [9-11]. The boundary data is specified from the near-source module on a cylindrical surface at $r = r_0$ from the pile, i.e. section 2.2.1, are used as input to the far-from-source module via the BEM.

The fundamental solutions of Green's displacement tensors $\widetilde{U}^{\Xi\xi}_{\alpha\beta}(\boldsymbol{r},\boldsymbol{r}_0,\omega)$ are derived from the potential functions [12] given the receiver point at $\boldsymbol{r} = (r,z)$ (in medium Ξ) in α-direction due to a unit impulse at source $\boldsymbol{r}_0 = (r_0,z_0)$ (in medium ξ) in β-direction:

$$\begin{aligned}\widetilde{U}^{s\xi}_{\alpha\beta}(\boldsymbol{r},\boldsymbol{r}_0,\omega) &= \nabla\tilde{\phi}^{g}_{s_j,\xi}(\boldsymbol{r},\boldsymbol{r}_0,\omega) + \nabla\times W, \quad W = -\frac{\partial\psi^{g}_{s_j,\xi}(\boldsymbol{r},\boldsymbol{r}_0,\omega)}{\partial r} \\ \widetilde{U}^{f\xi}_{\alpha\beta}(\boldsymbol{r},\boldsymbol{r}_0,\omega) &= \nabla\tilde{\phi}^{g}_{f,\xi}(\boldsymbol{r},\boldsymbol{r}_0,\omega)\end{aligned} \tag{14}$$

For the elastic domain, the Green's stress tensors $\widetilde{T}^{\Xi\xi}_{\alpha\beta}(\boldsymbol{r},\boldsymbol{r}_0,\omega)$ related to $\widetilde{U}^{\Xi\xi}_{\alpha\beta}(\boldsymbol{r},\boldsymbol{r}_0,\omega)$ can be obtained through substitution of Eq. (14) into the constitutive equations [12]. The fundamental solution pair $\{\widetilde{U}_{\alpha\beta},\widetilde{T}_{\alpha\beta}\}$ can be obtained once the unknown source strengths $S^{\xi}_{\beta}(\omega)$ are determined. By employing the Green's displacement tensors in Eq.(14), the traction vector can be expressed through stress tensor as,

$$\tilde{\tau}_i = \tilde{\sigma}_{ij} n_j \tag{15}$$

where $\tilde{\tau}_i$ is the traction vector in i direction, n_j is the unit normal vector at the boundary. The condition of a unit impulsive load can be applied in the β-direction at the source $\boldsymbol{r} = \boldsymbol{r}_0$ by setting, :

$$\begin{bmatrix}\tilde{\tau}_\beta \\ \tilde{\tau}_\alpha\end{bmatrix} = \begin{bmatrix}\delta(\boldsymbol{r}-\boldsymbol{r}_0) \\ 0\end{bmatrix} \tag{16}$$

The solution of Eq.(16) yields the coefficients $S^{p}_{\beta}(\omega)$ and $S^{s}_{\beta}(\omega)$.

For the acoustic domain, the conventional boundary integral representation is the Helmholtz integral in terms of pressure or displacement potential. By taking the directional derivative of the displacement potential as stated in Eq.(14), the boundary integral formulation for the displacement can be obtained directly by setting $S^f(\omega) = 1$, which is analogous to the integral formulation in the soil.

By utilizing Betti's reciprocal theorem in elastodynamics [10] and Green's theorem for acoustic problem [11], the complete solution for the acousto-elastic domain reads:

$$\begin{aligned}\tilde{u}_\alpha^\Xi(\boldsymbol{r}) = &\sum_{\beta=r,z}\int_{S^s}\left(\widetilde{U}_{\alpha\beta}^{\Xi s}(\boldsymbol{r},\boldsymbol{r}_0,\omega)\cdot\tilde{t}_\beta^{\boldsymbol{n}}(\boldsymbol{r}_0,\omega) - \widetilde{T}_{\alpha\beta}^{\boldsymbol{n},\Xi s}(\boldsymbol{r},\boldsymbol{r}_0,\omega)\cdot\tilde{u}_\beta(\boldsymbol{r}_0,\omega)\right)dS_0^s(\boldsymbol{r}_0)\\ &+\int_{S^f}\left(\widetilde{U}_{\alpha r}^{\Xi f}(\boldsymbol{r},\boldsymbol{r}_0,\omega)\cdot\tilde{p}(\boldsymbol{r}_0,\omega) - \widetilde{T}_{\alpha r}^{\boldsymbol{n},\Xi f}(\boldsymbol{r},\boldsymbol{r}_0,\omega)\cdot\tilde{u}_r(\boldsymbol{r}_0,\omega)\right)dS_0^f(\boldsymbol{r}_0), \quad \boldsymbol{r}\in V\end{aligned} \tag{17}$$

where $\boldsymbol{n}$ is the outward normal to the cylindrical boundary. The superscripts of the Green's tensors, "f" and "s" indicate fluid and soil domains, respectively.

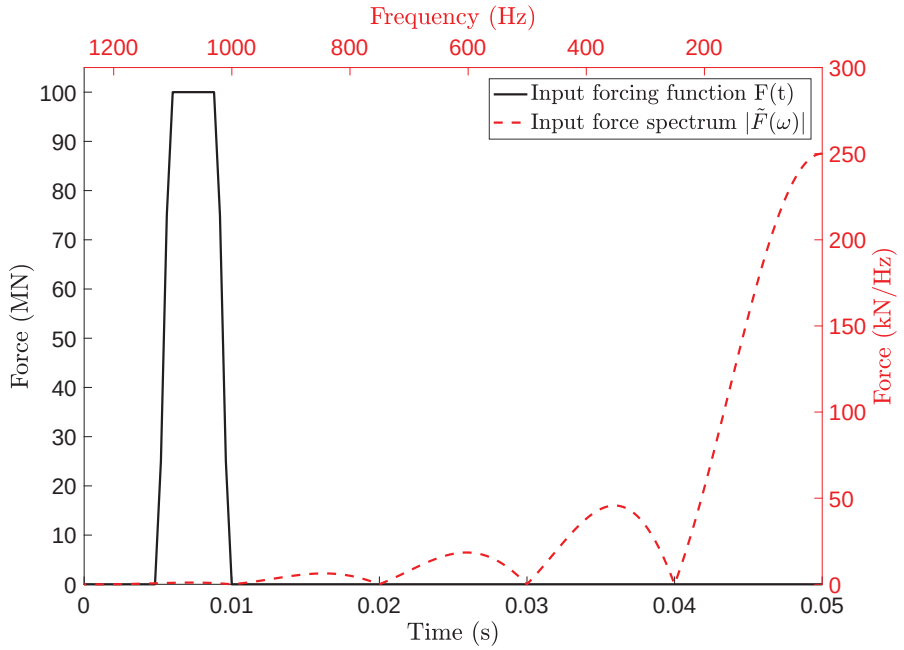

Figure 2: Input forcing function.

3 VALIDATION CASE STUDY

In order to validate the model, a benchmark case is considered with the measurement data recorded at offshore wind farm BARD Offshore 1 [5]. The material properties and the geometry of the model are given in Table 3 [5]. The seabed in the model consists of a thin marine sediment layer overlaying a stiffer soil half-space. The actual penetration depth of the pile was around 20 m. The pile was driven by a hydraulic hammer. The time signature of the applied force is the one shown in Fig.2, which generates approximately 1370 KJ blow energy into the system. The frequency spectrum is also given in Fig.2.

The peak pressure level (L_{peak}) and the sound exposure level (SEL) of receiver points at radial distances up to 1500m are shown in Fig.3. As can be seen, the difference between the

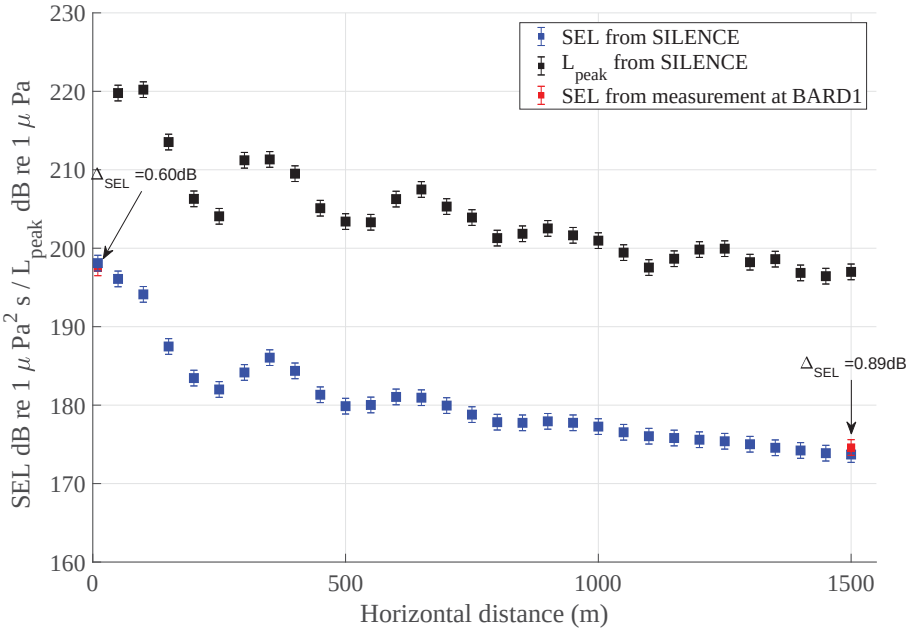

Figure 3: Comparison of SEL and L_{peak} at several radial distances from the pile and 2 m above the seabed.

Parameter	Pile	Parameter	Fluid	Upper soil	Bottom sediment
Length[m]	85	Depth [m]	40	2	48
Density [kg/m^3]	7850	ρ[kg/m^3]	1000	1888	1908
Outer diameter [m]	3.35	c_L [m/s]	1500	1705	1725
Wall thickness [mm]	70	c_T [m/s]	-	186	370
Final penetration depth [m]	20	α_p $[dB/\lambda]$	-	0.91	0.88
Maximum Blow Energy [kJ]	1370	α_s $[dB/\lambda]$	-	1.86	2.77

Table 1: Basic input parameters for the simulations.

predicted SEL and the measured values are 0.60 dB and 0.89 dB at 10m and 1500m radial distances from the pile respectively. The SEL indicates the averaged amount of energy radiated into the surrounding media and L_{peak} evaluates the impulsiveness of the pressure waves from the pile. The results verify the validity of the developed model, which can provide predictions that lies within the accuracy of the measurement equipment ($\pm$ 1 or 2 dB).

Figure 4 shows the pressure levels (dB re $1\mu Pa^2$/Hz) in 1/3-octave bands at various radial distances from the pile. Assuming that the energy in all the defined bandwidths (one-third octave) results from an effective source, the bandwidth energies add directly to give the total energy in one frequency band. The derivation of the sound pressure level in the unit of dB re 1 $\mu Pa^2 s^{-1}$ reads:

$$\mathrm{SPL}_{1/3-octave} = 10\log_{10}\sum_{i=m}^{n}\left(\frac{|\tilde{p}_i(\omega)|^2}{p_0^2}\right) \tag{18}$$

As can be seen in Fig.4, the spectrum shows that most of the energy is distributed at low frequencies, which is consistent with the 1/3-octave band spectrum obtained by measurement data and numerical results from FE-PE model in [5].

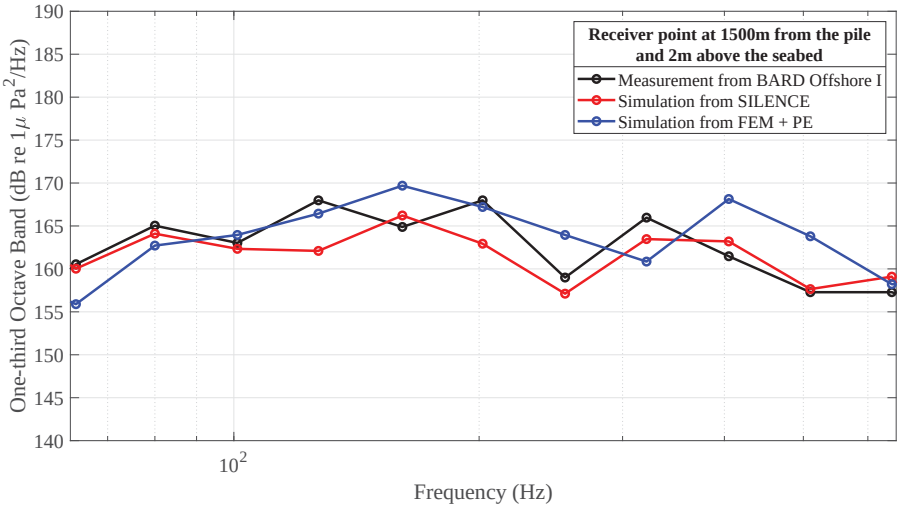

Figure 4: One-third octave band spectrum for a point positioned 2m above the seabed in the fluid and at r = 1500m from the pile.

4 CONCLUSIONS

The paper presents a computationally efficient coupled approach for noise predictions by offshore pile driving. The mathematical background of the generation and propagation of the sound field is given and the adopted method of solution is described. The direct boundary integral equation (BIE) formulation is adopted to propagate the radiated wave field from the near-source module to larger distances. A numerical analysis of a benchmark case is conducted, which verifies the validity of the model for the prediction of underwater noise from offshore pile driving. In the future, model predictions will be benchmarked against both numerical model predictions and available data from other measurement campaigns published in the scientific literature.

5 ACKNOWLEDGEMENTS

The authors gratefully acknowledge the China Scholarship Council (CSC) for financing this research project on the development of a generic underwater noise prediction model for offshore activities.

REFERENCES

[1] H. Bailey, B. Senior, D. Simmons, J. Rusin, G. Picken, and P. M. Thompson, Assessing underwater noise levels during pile-driving at an offshore windfarm and its potential effects on marine mammals, *Marine Pollution Bulletin*, 2010.

[2] P. G. Reinhall and P. H. Dahl, Underwater Mach wave radiation from impact pile driving: Theory and observation, *The Journal of the Acoustical Society of America*, vol. 130, pp. 1209–1216, sep 2011.

[3] T. Lippert and O. von Estorff, The significance of parameter uncertainties for the prediction of offshore pile driving noise, *The Journal of the Acoustical Society of America*, vol. 136, no. 5, pp. 2463–71, 2014.

[4] S. Lippert, M. Nijhof, T. Lippert, D. Wilkes, A. Gavrilov, K. Heitmann, M. Ruhnau, O. von Estorff, A. Schafke, I. Schafer, J. Ehrlich, A. MacGillivray, J. Park, W. Seong, M. A. Ainslie, C. de Jong, M. Wood, L. Wang, and P. Theobald, COMPILE—A Generic Benchmark Case for Predictions of Marine Pile-Driving Noise, *IEEE Journal of Oceanic Engineering*, vol. 41, pp. 1061–1071, 2016

[5] M. B. Fricke and R. Rolfes, Towards a complete physically based forecast model for underwater noise related to impact pile driving, *The Journal of the Acoustical Society of America*, 2015.

[6] A. Tsouvalas and A. V. Metrikine, A three-dimensional vibroacoustic model for the prediction of underwater noise from offshore pile driving, *Journal of Sound and Vibration*, vol. 333, no. 8, pp. 2283–2311, 2014.

[7] A. Tsouvalas and A. Metrikine, Structure-Borne Wave Radiation by Impact and Vibratory Piling in Offshore Installations: From Sound Prediction to Auditory Damage, *Journal of Marine Science and Engineering*, vol. 4, p. 44, 2016.

[8] A. Tsouvalas, K. N. van Dalen, and A. V. Metrikine, The significance of the evanescent spectrum in structure-waveguide interaction problems, *The Journal of the Acoustical Society of America*, 2015.

[9] A. A. Bakr, *Axisymmetric Potential Problems*, pp. 6–38. Berlin, Heidelberg: Springer Berlin Heidelberg, 1986.

[10] D. E. Beskos, Boundary element methods in dynamic analysis, *Applied Mechanics Reviews*, vol. 40, no. 1, pp. 1–23, 1987.

[11] F. Jensen, W. Kuperman, M. Porter, and H. Schmidt, *Computational Ocean Acoustics*, Springer New York, 2011.

[12] J. D. Achenbach, *Wave propagation in elastic solids*. North-Holland series in applied mathematics and mechanics, v. 16, Amsterdam New York: North-Holland Pub. Co.; American Elsevier Pub. Co., 1973.